

A Maximum Power Point Tracking Method Based on Perturb-and-Observe Combined With Particle Swarm Optimization

K. L. Lian, *Member, IEEE*, J. H. Jhang, and I. S. Tian

Abstract—Conventional maximum power point tracking (MPPT) methods such as perturb-and-observe (P&O) method can only track the first local maximum point and stop progressing to the next maximum point. MPPT methods based on particle swarm optimization (PSO) have been proposed to track the global maximum point (GMP). However, the problem with the PSO method is that the time required for convergence may be long if the range of the search space is large. This paper proposes a hybrid method, which combines P&O and PSO methods. Initially, the P&O method is employed to allocate the nearest local maximum. Then, starting from that point on, the PSO method is employed to search for the GMP. The advantage of using the proposed hybrid method is that the search space for the PSO is reduced, and hence, the time that is required for convergence can be greatly improved. The excellent performance of the proposed hybrid method is verified by comparing it against the PSO method using an experimental setup.

Index Terms—Global optimization, maximum power point tracking (MPPT), photovoltaic (PV) array, partial shading.

I. INTRODUCTION

OVER the few past decades, many algorithms to track the maximum power point (MPP) have been proposed. Among these, perturb-and-observe (P&O), hill-climbing (HC), and incremental conductance (INC) are the most widely used methods [1]–[3]. As shown in [4] and [5], these methods are essentially different ways of envisioning the same fundamental concept, and rely on determining the gradient of the power with respect to the current or voltage using the perturbation method in each iteration. When the first local maximum point (LMP) is reached, the algorithms stop progressing to the next maximum point (if there is any). Consequently, the main drawback of these methods is that they tend to converge to a single LMP, which is only appropriate under uniform insolation conditions.

Under partially shaded conditions, the shaded cells in a module become reverse biased and behave as a load, leading to the

hot spot problem. To avoid this, bypass diodes are used to conduct the current that is generated by the nonshaded cells within a module. However, the connection of bypass diodes will change the uniform current–voltage (I – V) and power–voltage (P – V) characteristics of the module, resulting in multiple peaks [6]. To maximize the efficiency of the module, it is necessary to track the global maximum point (GMP). Two approaches are generally used to reduce or counteract the shading effect. The first is based on hardware fixtures, such as adaptive reconfiguration schemes for the PV arrays [7] and multilevel converter systems [8] that allow each PV source to be controlled separately. This approach is complex and costly [9]. The second approach is to track the GMP by developing advanced control algorithms, and this will be the focus of this paper.

Kobayashi *et al.* [10] have proposed a two-stage method to track the GMP. In the first stage, the operating point of the photovoltaic (PV) system moves into the vicinity of the GMP by estimating the equivalent load line. Then, the INC method is employed to converge to the MPP in the second stage. Because the equivalent load line in the first stage is estimated under uniform insolation conditions, some partial shading conditions (PSCs) may cause an LMP to be tracked in the second stage [11]. In [9], a scanning process is first utilized to detect the regions which contain the GMP. After that, a P&O algorithm is used to find the GMP. Although this method can successfully find the GMP, the tracking speed is limited because almost all LMPs must be found and compared to obtain the GMP. A Fibonacci search (FS) method was proposed in [12]. However, as this is a linear search method, a GMP still cannot be guaranteed. The “DIRECT” (dividing rectangles) algorithm, which is proposed in [7], is based on a Lipschitz condition to find the maximum point. To ensure that the GMP is found, the search areas to be divided must be selected with care; otherwise, false GMP may be found. Lei *et al.* [13] proposed a sequential extremum seeking control strategy for GMP tracking. However, this process requires the variation bound for the turning-point voltage to be found. This in turn requires knowledge of the P – V or P – I characteristics under variable-shading circumstances, which may be difficult to obtain in practice. Researchers have also used artificial intelligence algorithms to develop maximum power point tracking (MPPT) methods. In [6], a radial basis function and a three-layered feedforward neural network are used to track the GMP. However, the accuracy of this scheme depends on the volume of training data, and considerable computational effort is needed to ensure reliability and accuracy under any shading condition.

Manuscript received February 2, 2013; revised August 10, 2013; accepted December 23, 2013. Date of publication January 16, 2014; date of current version February 17, 2014. This work was supported by the National Science Council under Contract NSC 101-2221-E-011-119.

K. L. Lian and J. H. Jhang are with the Power and Energy Group, National Taiwan University of Science and Technology, Taipei City 10607, Taiwan (e-mail: kllian@mouse.ee.ntust.edu.tw; b9707110@mail.ntust.edu.tw).

I. S. Tian is with MiTAC International Corp., Taipei 11568, Taiwan (e-mail: sankigood@hotmail.com).

Color versions of one or more of the figures in this paper are available online at <http://ieeexplore.ieee.org>.

Digital Object Identifier 10.1109/JPHOTOV.2013.2297513

Chen *et al.* [14] demonstrated an MPPT method that is based on biological swarm chasing behavior to increase the tracking performance. Nevertheless, only uniform insolation conditions were considered and PSCs were not addressed. Miyatake *et al.* [15] have realized centralized MPPT control of modular PV systems, and used particle swarm optimization (PSO) to determine the individual module voltage. They showed that PSO can outperform conventional methods such as HC and FS under PSCs. Ishaque *et al.* [16] and Liu *et al.* [17] implemented PSO-based MPPT control algorithms in a PV system, consisting of a high-power single-stage converter. However, as reported in [18], one problem of the PSO algorithm is the long GMP tracking time for large search spaces. In [18], the authors proposed to remove the random number from the PSO acceleration factors to reduce the tracking time. Nevertheless, the value of the maximum change in the particle velocity must be restricted; otherwise, LMPs may be obtained. Moreover, Ishaque and Salam [18] gave no guidelines on how to select this value.

This paper proposes a hybrid of the P&O and PSO methods. Initially, the P&O method is employed to identify the nearest local maximum. Starting from that point, the PSO method is used to search for the GMP. The advantage of this hybrid method is that the search space of the PSO is reduced, and hence, the time required for convergence can be greatly decreased. Moreover, there is no need to place a restriction on the maximum particle velocity. The rest of this paper is arranged as follows. The PSO method will be briefly reviewed in Section II. Section III then describes the proposed method. The experimental setup and a comparison of PSO and the proposed hybrid method are described in Section IV. Finally, the paper is concluded in Section V.

II. REVIEW OF THE PARTICLE SWARM OPTIMIZATION METHOD

In this paper, a voltage-based controller will be discussed. The PV voltage as the regulated variable is easier to implement because the MPPT controller can quickly decide the initial points according to the percentage of the open-circuit voltage (V_{oc}) [19]. In addition, current-based control implementation requires caution to prevent the PV current to reach its short-circuit current, I_{sc} , resulting in sudden voltage drop and causing power losses [19]. In [19] and [20], a detailed discussion on the comparison of voltage- and current-based MPPT controllers is provided.

The PSO method is a metaheuristic approach [21] that can be applied to optimize a function which is difficult or impossible to express analytically. The PSO algorithm can be expressed mathematically by two equations which specify the velocity and position update of a particle i

$$u_i^{k+1} = \omega u_i^k + c_1 r_1 (p_{besti} - x_i^k) + c_2 r_2 (g_{best} - x_i^k) \quad (1)$$

$$x_i^{k+1} = x_i^k + u_i^{k+1} \quad (2)$$

where u_i^k is the velocity of individual i at iteration k , ω is an inertia weight parameter, c_1 and c_2 are acceleration coefficients, r_1 and r_2 are random numbers between 0 and 1, x_i^k is the position of individual i at iteration k , p_{besti} is the best position of individual i at iteration k , and g_{best} is the best position of the

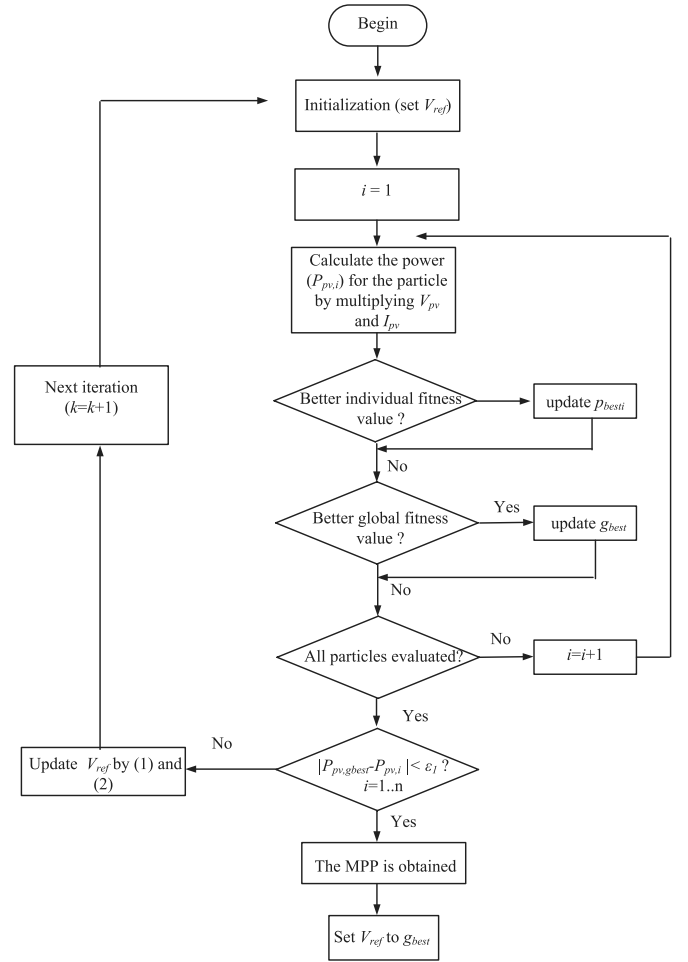


Fig. 1. Flowchart for the PSO method.

group up to iteration k . The value of ω can be determined by an equation or set to a fixed value. The purpose of the MPPT block is to obtain V_{ref} , which is sent to the PI controller. Therefore, the position (x) variables in (1) and (2) are actually the voltage references (V_{ref}), whereas the velocity (u) variables can be regarded as the correction terms for the voltage references. Since the converter can only respond to one command at a time, the particles are initialized and evaluated in a successive manner. The interval between successive particles, T_{int} , must be greater than the settling time of the system in order to obtain correct current and voltage samples [6], [17]. Fig. 1 summarizes the control action of the PSO method used for MPPT. In the first iteration, V_{ref} is initially set to some value (see Section IV-B). It is then updated according to (1) and (2). The power $P_{pv,i}$ is calculated by multiplying the measured voltage (V_{pv}) and current (I_{pv}). Then, the algorithm proceeds to check whether this voltage reference value will result in a better individual fitness value [17] by evaluating the following equation:

$$P_{pv,i} > P_{pv,i-1}. \quad (3)$$

If (3) is satisfied, the individual fitness value (p_{besti}) is updated; otherwise, p_{besti} retains its present value. $P_{pv,i}$ is then checked against the power of the other particles to see if the global fitness

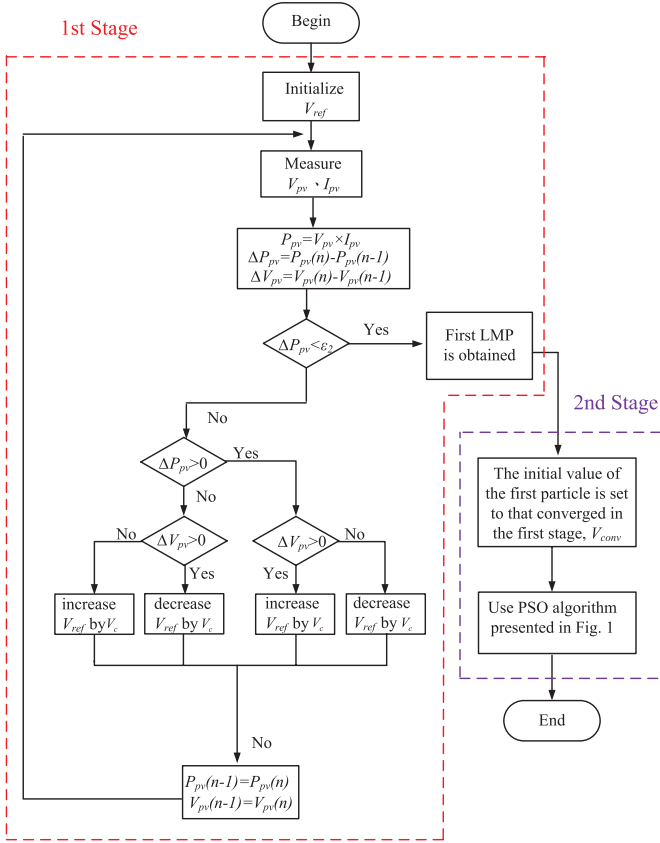


Fig. 2. Flowchart for the proposed method.

value (g_{best}) requires updating. A sufficient amount of time must be provided for each particle to perform all the aforementioned steps. Finally, the convergence criterion as defined in (4) is checked to ensure that all the particles converge to the GMP

$$|P_{pv,gbest} - P_{pv,i}| < \varepsilon_1; i = 1 \dots n \quad (4)$$

where ε_1 is the tolerance value.

III. PROPOSED METHOD

Fig. 2 illustrates the proposed hybrid algorithm as a flowchart. The method consists of two stages. In the first stage, the P&O method is employed to quickly search for the first local maximum. The operating voltage (V_{pv}) is perturbed by a small amount (V_c) [19], [22] every control cycle (T_{perb}) to determine whether the algorithm is traveling up or down in the P - V curve. Note that a convergence criterion ($\Delta P_{pv} < \varepsilon_2$) needs to be introduced in the first stage of the proposed method, as shown in Fig. 2 to locate the first LMP and to pass it to the second stage. The value of ε_2 should be chosen with care because if it is too large, the program may switch to the second stage before reaching the first LMP. On the other hand, if it is too small, the time staying in the first stage may be long before proceeding to the second stage. Although ε_2 may be obtained by trial and error, it can also be obtained by a systematic procedure, as suggested in [23] and [24]. This is especially useful when oscillations occur in the voltage of the energy storage capacitor because the program needs to distinguish variations in the

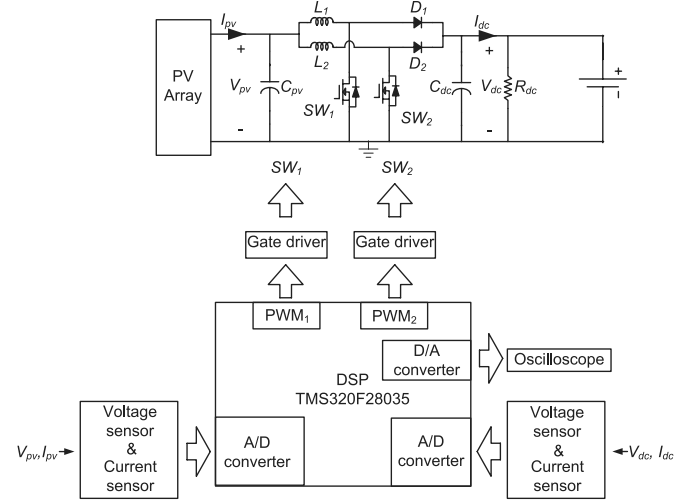


Fig. 3. Schematic diagram of the PV system.

operating point induced by the perturbation from those caused by the disturbance coming from capacitor voltage ripples.

In the second stage, the PSO is activated to search for the GMP. The initial condition of the first particle is set to the converged value from the first stage V_{conv} . The initial conditions of the other $(n - 1)$ particles are set to values ranging from V_{conv} to the upper bound of the search space. Because the number of particles remains the same but the search space is smaller, the hybrid method is expected to find the GMP in a shorter time than that taken by the PSO method alone.

It is worth noting that P&O is chosen because of its ease of implementation. However, HC and INC could easily be applied in the proposed method. Moreover, variable-step P&O, HC, and INC methods have been proposed to minimize the effects of oscillations at the MPP. However, these methods are not used in the proposed hybrid method because once the first LMP is detected by the P&O method, it will switch to the second stage, and the final MPP will be obtained by means of the PSO. Thus, the fixed-step P&O method is sufficient and will minimize the computational effort in the first stage.

IV. EXPERIMENTS AND VALIDATIONS

A. Configuration of the Experimental Setup

Fig. 3 shows the experimental setup of the PV system that is used to validate the proposed method. The PV array in the figure is realized by a programmable PV emulator that is manufactured by Chroma (Model 62150H-1000S Solar Array Simulator). This PV emulator is able to mimic the output of a photovoltaic installation exposed to various shading conditions. In this paper, three different cases are tested:

Case 1: This is the nonshading condition, and there is only one LMP, which is also the GMP. As shown in Fig. 4(a), the GMP occurs at (455 W, 174 V) on the P - V curve. The short-circuit current (I_{sc}) is 2.8 A, whereas the open-circuit voltage (V_{oc}) is 218.6 V.

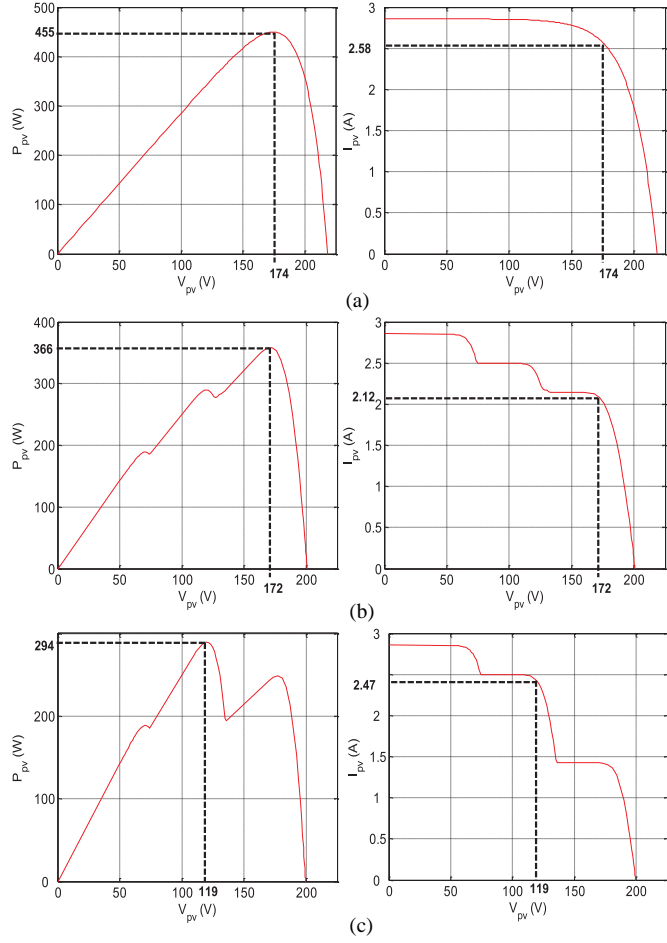


Fig. 4. (a) Case 1: The nonshading condition. (b) Case 2: There are three LMPs, and the GMP occurs at the rightmost one on the P - V curve. (c) Case 3: There are three LMPs, and the GMP does NOT occur at the rightmost one on the P - V curve.

Case 2: There are three LMPs, and the GMP occurs at the rightmost one on the P - V curve (i.e., close to the open-circuited voltage on the P - V curve). As shown in Fig. 4(b), the GMP occurs at (366 W, 172 V). In this case, $I_{sc} = 2.8$ A, and $V_{oc} = 201$ V.

Case 3: There are three LMPs, and the GMP does not occur at the rightmost of the P - V curve. As shown in Fig. 4(c), the GMP occurs at (294 W, 119 V). In this case, $I_{sc} = 2.8$ A, and $V_{oc} = 201$ V.

The dc-dc converter is a boost converter with an interleaved topology to reduce the ripple current, improve reliability, and increase efficiency [25]. The controller is implemented in a 32-bit digital signal processor (DSP-TMS320F28035), which sends out gating signals, PWM_1 and PWM_2 to the gate drivers to control the MOSFET switches (SW_1 and SW_2) in a complementary fashion. V_{pv} and I_{pv} are sent to the DSP via sensor circuits and A/D converters. The MPPT controller takes V_{pv} and I_{pv} and determines the voltage reference, which is then sent to the PI controller. The PI controller's proportional gain is -0.85 and its integral gain is 0.018 . The load is a resistive load whose voltage is regulated by a dc voltage source (Chroma programmable dc power supply 620120P-600-8). Thus, the load

TABLE I
PARAMETER VALUES OF THE CONVERTER CIRCUIT

Rated Input voltage	225 V
Rated Output voltage	400 V
Input current	0.6 – 5 A
Output current	0.6 – 2.8 A
Switching frequency	100 kHz
D_1, D_2	IQBD30E60A1
MOSFET switches	SPW35N60C3
Load	300 Ω
L_1, L_2	2 mH
C_{pv}, C_{dc}	470 μ F

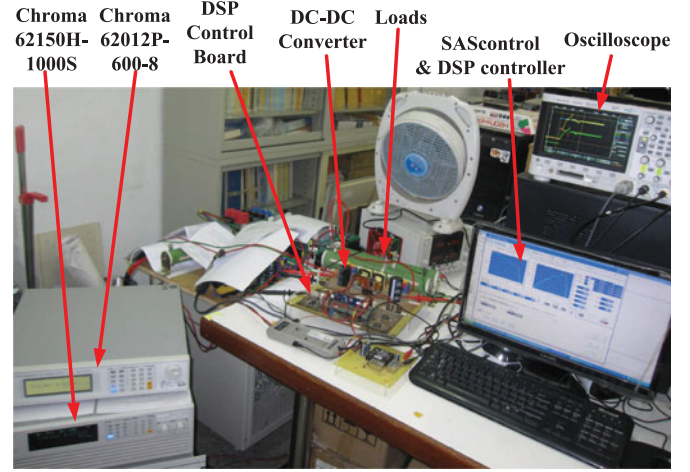


Fig. 5. Experimental setup of the PV system.

voltage is held at 400 V. Table I summarizes the parameter values of the converter circuit, and Fig. 5 shows the actual setup. Depending on the PV system application, a dc/dc power converter is used to interface the PV array output power to either a battery bank or a dc/ac inverter connected to the grid. Both of these types can be represented by Fig. 3.

B. Parameter Value Setting and Initial Conditions for the Proposed and Particle Swarm Optimization Algorithms

The parameter values of ω , c_1 , and c_2 of (1) used in the PSO and hybrid methods are 0.4, 1.5, and 1.5, respectively. Note that these values are determined via offline simulation for Case 1, and are used for the other two cases. The number of particles used is three due to the memory limitations of the DSP-TMS320F28035. In addition, Kobayashi *et al.* [10] have performed an optimization analysis and concluded that three particles actually yield the best performance.

Since iterative methods require an initial estimate, it is important to have a systematic method for determining the initial conditions. In general, an initial estimate closer to the MPP will result in faster convergence. However, it is usually not possible to know *a priori* the location of the MPP. As V_{oc} is usually given in the datasheet or can be directly measured, it is most convenient to set the initial conditions according to this value.

Consequently, the initial conditions for each case are set as follows:

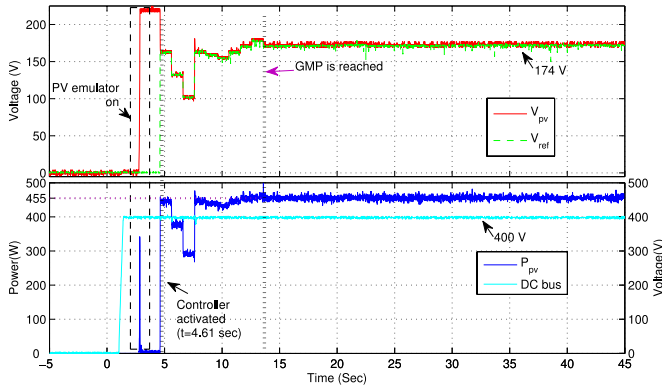


Fig. 6. Voltage and power waveforms of the PSO method for Case 1.

PSO: The initial value of the first particle is set to be 80% of V_{oc} . The initial values for the second and third particles are set to 65% and 50% of V_{oc} , respectively.

Hybrid: In the first stage, the initial value of V_{ref} is set to 80% of V_{oc} . In the second stage, once the PSO is activated, the initial condition of the first particle is set to the converged value from the first stage, V_{conv} . The initial values of the second and third particles are set to be 15% and 30% from the V_{conv} , respectively.

Taking into account the transient response and the command response times of the Chroma PV emulator, T_{perb} for the P&O interval (i.e., the first stage of the proposed method) is set to 0.1 s, and T_{int} for the PSO (also the second stage of the proposed method) is set to 1 s. These values are larger than the response time of the PV emulator to ensure reliable operation [17]. The values of T_{perb} and T_{int} can be scaled appropriately if actual PV panels are used.

C. Case Studies

To validate the proposed method and compare it with the PSO approach, the $V-I$ curves of each case, as described in Fig. 4, are imported to the PV emulator to study their tracking times and MPPT capabilities.

Case 1: In this case, there is only one MPP, which occurs at 455 W. Fig. 6 shows the voltage (upper plot) and power (lower plot) waveforms when the PSO method is employed for the MPPT. As can be seen from the voltage plot, V_{pv} closely tracks the voltage reference V_{ref} when the controller is activated at $t = 4.61$ s.¹ This demonstrates that the PI controllers function properly. However, it takes three cycles (9 s) for the PSO to reach the MPP. Note that a PSO cycle is the time required for the three particles to move. During the first PSO cycle, the three particles follow the initial values, which are assigned in Section IV-B. After the first PSO cycle, the reference values are calculated that are based on (1) and (2) for the remaining PSO cycles before reaching the MPP. On the other hand, Fig. 7 shows the current (upper plot) and power (lower plot) waveforms when the

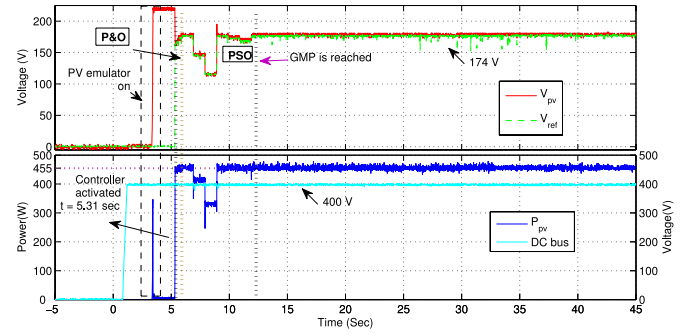


Fig. 7. Voltage and power waveforms of the proposed method for Case 1.

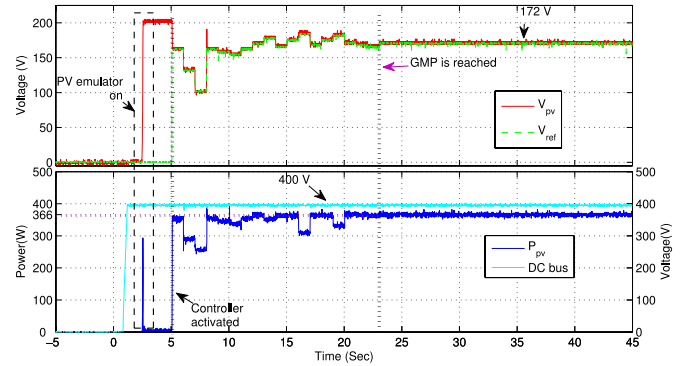


Fig. 8. Voltage and power waveforms of the PSO method for Case 2.

proposed method is employed. The controller is turned ON at $t = 5.31$ s. It takes about 6.59 s to reach the MPP. As observed in the figure, from $t = 5.31$ to 5.90 s, the P&O algorithm is employed, and the MPP is obtained. After the P&O interval, the proposed algorithm switches to the PSO search algorithm. The first particle takes the converged value from the P&O interval, which is about 177 V. The second particle is 150 V, and the third particle is 124 V. They only take two cycles to reach the MPP because the search space is smaller.

Case 2: In this case, the first LMP, which also happens to be the GMP, occurs at 366 W. The voltage at the GMP is 172 V. Fig. 8 shows the voltage and power waveforms when the PSO method is employed. It takes six PSO cycles (18 s) to reach the GMP, which is longer than in Case 1. This is reasonable because the number of local optima strongly affects the convergence rate [26]. Consequently, it will take more time for all the particles to converge to the final value (i.e., MPP) in Case 2. Fig. 9 shows the voltage and power waveforms of the proposed method. It takes only 9.69 s to reach the GMP. As shown in the figure, the first LMP is located via the P&O method. The solution oscillates around that point very briefly, before switching to the PSO algorithm at $t = 5.87$ s. It then takes only three PSO cycles to reach the GMP, exhibiting a much shorter convergence time than that of the conventional PSO algorithm. This is because the search space for the GMP is reduced by the P&O method, allowing the three particles to converge to the GMP much faster.

Case 3: In this case, the GMP is about 294 W and occurs in the middle portion of the $P-V$ curve. Fig. 10 shows the voltage and power waveforms when the PSO is employed for MPPT.

¹Note that prior to the activation of the controller, the dc voltage source at the load side has already been turned ON, keeping the load voltage at 400 V, as shown in Figs. 6–15.

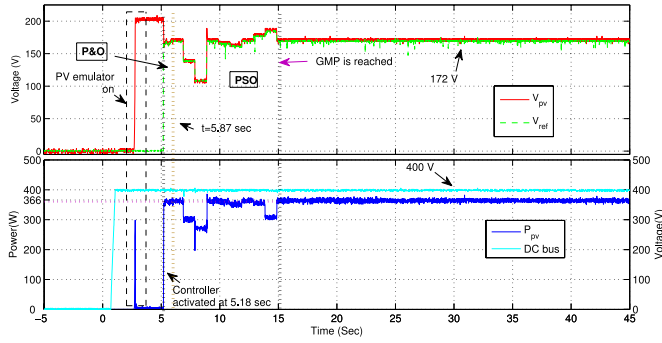


Fig. 9. Voltage and power waveforms of the proposed method for Case 2.

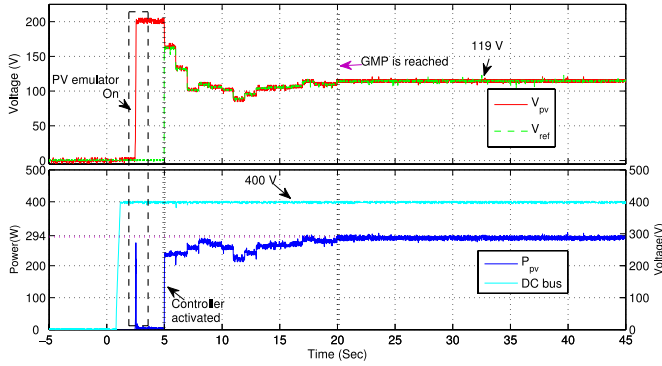


Fig. 10. Voltage and power waveforms of the PSO method for Case 3.

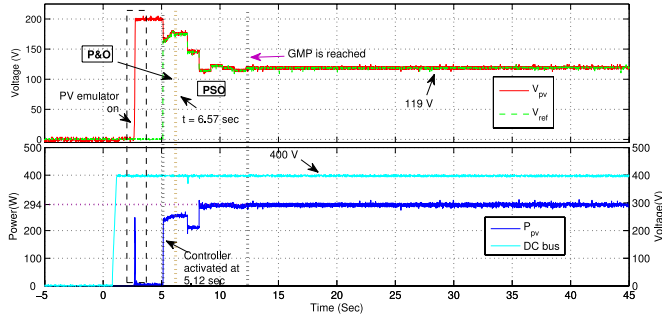


Fig. 11. Voltage and power waveforms of the proposed method for Case 3.

Similar to the previous cases, the three particles are assigned initial values of 161, 131, and 101 V. It then takes five PSO cycles (15 s) to reach the GMP. In comparison, it takes 7.45 s to reach the GMP using the proposed method. As shown in Fig. 11, the first LMP is identified by the P&O algorithm at $t = 6.57$ s. After switching to the PSO algorithm, two PSO cycles are needed for the solution to converge. It can be seen that the proposed method outperforms the PSO method because the third particle is already at the vicinity of the first LMP only 3.10 s after the controller is activated at $t = 5.12$ s. On the other hand, for the conventional PSO method, it takes 12 s to reach the vicinity of the first LMP.

In all three cases, both the PSO and proposed methods can successfully track the GMPs. The proposed hybrid method reaches the GMP faster than the PSO method in each case. In terms of the computational burden, the proposed method requires almost the same number of operations (slightly fewer)

as PSO. This is evident from Table II, which lists the number of mathematical operations (additions and multiplications) required for Cases 1 to 3 for a period of 30 s after the controller is turned ON. This interval was chosen because, by that time, both methods reach steady-state conditions in all three cases.

D. Variations of Partial Shading

To investigate the dynamic tracking capability, the changing sequences of the shaded patterns are investigated for two scenarios. In the first scenario, the sequence is changed from Case 1 to 2 and from 2 to 3, whereas in the second scenario, the sequence is changed from Case 3 to 1 and from 1 to 2. The two scenarios illustrate the dynamic performance of the two methods when the level of (P_{pv}) changes from high to low and from low to high. In addition, the connections of these GMPs cannot be approximated as a straight line, which makes the tracking process challenging. To achieve this, the following constraints [17] are used to detect whether the GMP has changed:

$$\frac{|P_{pv} - P_{pv,last}|}{P_{pv,last}} \geq \Delta P(\%) \quad (5)$$

where $P_{pv,last}$ represents the DC power at the GMP of the last operating point, and ΔP is set to 10%. Note that this value, as shown in [23], needs to be greater than the power variations caused by the P&O perturbation. Femia *et al.* [23] also show how a theoretical optimized value can be obtained. If (5) is satisfied, all the particles are reinitialized to search for the new GMP.

Figs. 12 and 13 show the voltage and power waveforms of the PSO and proposed methods, respectively, caused by the shading pattern of the first scenario. The controller is activated at approximately $t = 6.0$ s. It takes about 9 s (three PSO cycles) and 4.10 s (1.10 s for the P&O + one PSO cycle) for the PSO and proposed methods, respectively, to reach the first GMP. Then, at around $t = 29$ s, the P - V curves changes to that of Case 2 [as described in Fig. 4(b)]. It takes 18 s (six PSO cycles) and 6.98 s (0.98 s for the P&O + two PSO cycles) for the PSO and proposed methods, respectively, to reach the GMP. Finally, at around $t = 69$ s, the PV pattern changes to that of Case 3 [as described in Fig. 4(c)], and takes about 15 s (five PSO cycles) and 6.62 s (0.62 s for P&O + two PSO cycles) for the PSO and proposed methods, respectively, to reach the corresponding GMP.

Figs. 14 and 15 show the voltage and power waveforms of the PSO and proposed methods, respectively, for the second scenario. The controller is activated at around $t = 6.0$ s. It takes about 15 s (five PSO cycles) and 6.71 s (0.71 s for P&O + two PSO cycles) for the PSO and proposed methods, respectively, to reach the first GMP. Then, at around $t = 43$ s, the PV curves change to that of Case 1. It takes 9 s (three PSO cycles) and 7.22 s (1.22 s for P&O + two PSO cycles) for the PSO and proposed methods, respectively, to reach the GMP. Finally, at around $t = 69$ s, the PV pattern changes to that of Case 2, and takes about 21 s (seven PSO cycles) and 9.88 s (0.88 s for P&O + three PSO cycles) for the PSO and proposed methods, respectively, to reach the corresponding GMP.

TABLE II
NUMBER OF MATHEMATICAL OPERATIONS FOR A PERIOD OF 30 S AFTER THE CONTROLLER IS SWITCHED ON

Method	Case 1			Case 2			Case 3		
	No. of +	No. of ×	Total	+	No. of ×	Total	No. of +	No. of ×	Total
PSO	223	181	404	223	181	404	223	181	404
Hybrid	208	173	381	209	174	383	214	178	392

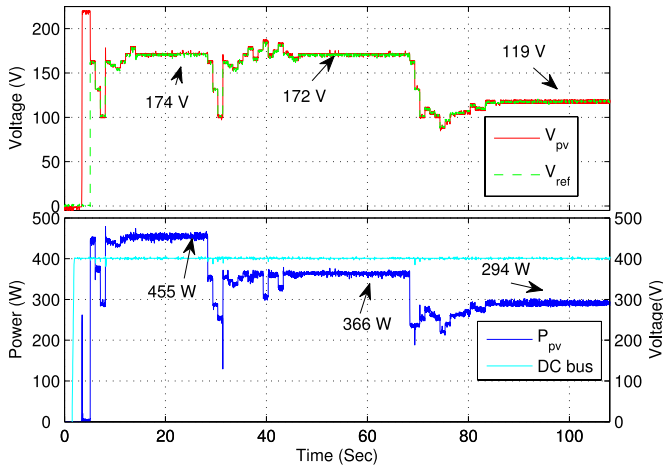


Fig. 12. Voltage and power waveforms of the PSO method for variations of partial shading (Scenario 1).

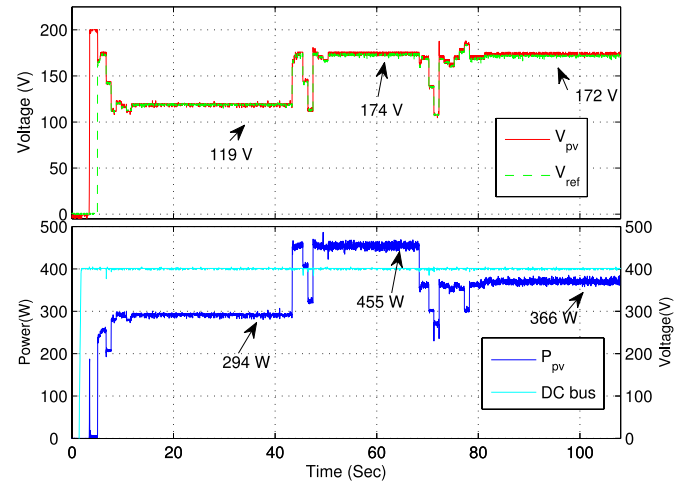


Fig. 15. Voltage and power waveforms of the proposed method for variations of partial shading (Scenario 2).

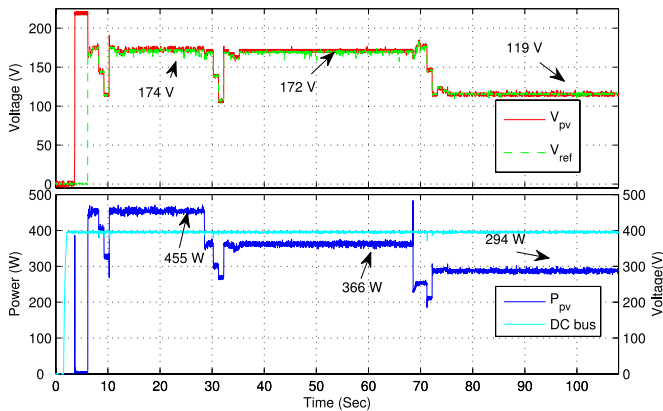


Fig. 13. Voltage and power waveforms of the proposed method for variations of partial shading (Scenario 1).

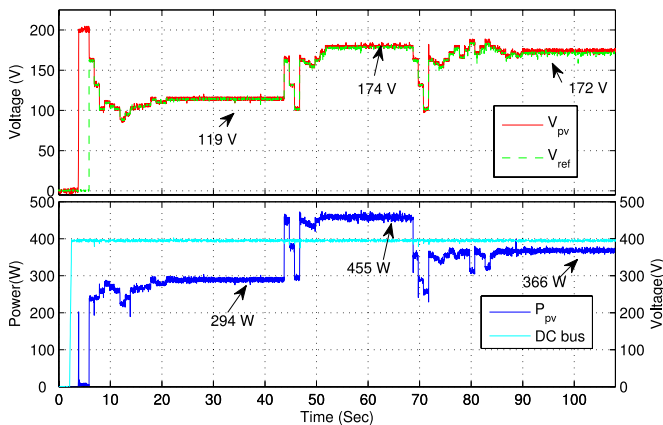


Fig. 14. Voltage and power waveforms of the PSO method for variations of partial shading (Scenario 2).

These two tests effectively demonstrate that the proposed method can track the GMP dynamically, requiring less time and exhibiting fewer voltage oscillations during the transients than the PSO method (see Figs. 13 and 15).

Finally, some preliminary continuous dynamic tests such as the trapezoidal irradiance test profiles in EN 50530 standard have been done and the proposed method still yields better performance. Nevertheless, due to the limited space, this will be addressed in detail in a future paper.

V. CONCLUSION

This paper described a new MPPT method that can be used to track the GMP when a PV panel is partially shaded by clouds, snow, trees, and/or buildings. The proposed approach essentially combines P&O and PSO to form a hybrid method. In the first stage, the P&O method is employed to quickly search for the first LMP. Then, in the second stage, the PSO is used to search for the GMP. The search space in the second stage is reduced, allowing the GMP to quickly be obtained. Experimental results show that the proposed hybrid method can track the GMP with no problem, and has a faster convergence time and better dynamic response than the plain PSO method.

ACKNOWLEDGMENT

The authors would like to sincerely thank the editor, anonymous reviewers, Dr. J. Bloemink from Powertech Labs, Inc., Prof. P.-T. Cheng from National Tsing Hua University, and Prof. P. Lehn from University of Toronto for their valuable comments and suggestions, which improved the quality of the paper.

REFERENCES

- [1] A. Bidram, A. Davoudi, and R. Balog, "Control and circuit techniques to mitigate partial shading effects in photovoltaic arrays," *IEEE J. Photovoltaics*, vol. 2, no. 4, pp. 532–546, Oct. 2012.
 - [2] A. Safari and S. Mekhilef, "Simulation and hardware implementation of incremental conductance MPPT with direct control method using Cuk converter," *IEEE Trans. Ind. Electron.*, vol. 58, no. 4, pp. 1154–1161, Apr. 2011.
 - [3] T. K. Soon, S. Mekhilef, and A. Safari, "Simple and low cost incremental conductance maximum power point tracking using buck-boost converter," *J. Renewable Sustainable Energy*, vol. 5, no. 2, pp. 0 231 061–02 310 612, 2013.
 - [4] S. Kjaer, "Evaluation of the hill climbing and the incremental conductance maximum power point trackers for photovoltaic power systems," *IEEE Trans. Energy Convers.*, vol. 27, no. 4, pp. 922–929, Dec. 2012.
 - [5] D. Sera, L. Mathe, T. Kerekes, S. Spataru, and R. Teodorescu, "On the perturb-and-observe and incremental conductance MPPT methods for PV systems," *IEEE J. Photovoltaics*, vol. 3, no. 3, pp. 1070–1078, Jul. 2013.
 - [6] Syafaruddin, E. Karatepe and T. Hiyama, "Artificial neural network-polar coordinated fuzzy controller based maximum power point tracking control under partially shaded conditions," *IET Renewable Power Generation*, vol. 3, no. 2, pp. 239–253, Jun. 2009.
 - [7] D. Nguyen and B. Lehman, "An adaptive solar photovoltaic array using model-based reconfiguration algorithm," *IEEE Trans. Ind. Electron.*, vol. 55, no. 7, pp. 2644–2654, Jul. 2008.
 - [8] I. Abdalla, J. Corda, and L. Zhang, "Multilevel dc-link inverter and control algorithm to overcome the PV partial shading," *IEEE Trans. Power Electron.*, vol. 28, no. 1, pp. 14–18, Jan. 2013.
 - [9] E. Koutroulis and F. Blaabjerg, "A new technique for tracking the global maximum power point of PV arrays operating under partial-shading conditions," *IEEE J. Photovoltaics*, vol. 2, no. 2, pp. 184–190, Apr. 2012.
 - [10] K. Kobayashi, I. Takano, and Y. Sawada, "A study on a two stage maximum power point tracking control of a photovoltaic system under partially shaded insolation conditions," in *Proc. IEEE Power Eng. Soc. General Meeting*, Jul. 2003, vol. 4, pp. 2612–2617.
 - [11] B. Alajmi, K. Ahmed, S. Finney, and B. W. Williams, "A maximum power point tracking technique for partially shaded photovoltaic systems in microgrids," *IEEE Trans. Ind. Electron.*, vol. 60, no. 4, pp. 1596–1606, Apr. 2013.
 - [12] M. Miyatake, T. Inada, I. Hiratsuka, H. Zhao, H. Otsuka, and M. Nakano, "Control characteristics of a Fibonacci-search-based maximum power point tracker when a photovoltaic array is partially shaded," in *Proc. Int. Power Electron. Motion Control Conf.*, Aug. 2004, vol. 2, pp. 816–821.
 - [13] P. Lei, Y. Li, and J. Seem, "Sequential ESC-based global MPPT control for photovoltaic array with variable shading," *IEEE Trans. Sustainable Energy*, vol. 2, no. 3, pp. 348–358, Jul. 2011.
 - [14] L.-R. Chen, C.-H. Tsai, Y.-L. Lin, and Y.-S. Lai, "A biological swarm chasing algorithm for tracking the PV maximum power point," *IEEE Trans. Energy Convers.*, vol. 25, no. 2, pp. 484–493, Jun. 2010.
 - [15] M. Miyatake, M. Veerachary, F. Toriumi, N. Fujii, and H. Ko, "Maximum power point tracking of multiple photovoltaic arrays: A PSO approach," *IEEE Trans. Aerospace Electron. Syst.*, vol. 47, no. 1, pp. 367–380, Jan. 2011.
 - [16] K. Ishaque, Z. Salam, M. Amjad, and S. Mekhilef, "An improved particle swarm optimization (PSO)-based MPPT for PV with reduced steady-state oscillation," *IEEE Trans. Power Electron.*, vol. 27, no. 8, pp. 3627–3638, Aug. 2012.
 - [17] Y.-H. Liu, S.-C. Huang, J.-W. Huang, and W.-C. Liang, "A particle swarm optimization-based maximum power point tracking algorithm for PV systems operating under partially shaded conditions," *IEEE Trans. Energy Convers.*, vol. 27, no. 4, pp. 1027–1035, Dec. 2012.
 - [18] K. Ishaque and Z. Salam, "A deterministic particle swarm optimization maximum power point tracker for photovoltaic system under partial shading condition," *IEEE Trans. Ind. Electron.*, vol. 60, no. 8, pp. 3195–3206, Aug. 2013.
 - [19] W. Xiao, N. Ozog, and W. Dunford, "Topology study of photovoltaic interface for maximum power point tracking," *IEEE Trans. Ind. Electron.*, vol. 54, no. 3, pp. 1696–1704, Jun. 2007.
 - [20] T. Suntio, J. Leppaaho, J. Huusari, and L. Nousiainen, "Issues on solar-generator interfacing with current-fed MPP-tracking converters," *IEEE Trans. Power Electron.*, vol. 25, no. 9, pp. 2409–2419, Sep. 2010.
 - [21] J. Kennedy and R. Eberhart, "Particle swarm optimization," in *Proc. IEEE Int. Conf. Neural Netw.*, Nov./Dec. 1995, vol. 4, pp. 1942–1948.
 - [22] M. Masoum, H. Dehbonei, and E. Fuchs, "Theoretical and experimental analyses of photovoltaic systems with voltage and current-based maximum power-point tracking," *IEEE Trans. Energy Convers.*, vol. 17, no. 4, pp. 514–522, Dec. 2002.
 - [23] N. Femia, G. Petrone, G. Spagnuolo, and M. Vitelli, "Optimization of perturb and observe maximum power point tracking method," *IEEE Trans. Power Electron.*, vol. 20, no. 4, pp. 963–973, Jul. 2005.
 - [24] N. Femia, G. Petrone, G. Spagnuolo, and M. Vitelli, "A technique for improving p and o MPPT performances of double-stage grid-connected photovoltaic systems," *IEEE Trans. Ind. Electron.*, vol. 56, no. 11, pp. 4473–4482, Nov. 2009.
 - [25] P. W. Lee, Y. S. Lee, D. K. W. Cheng, and X. C. Liu, "Steady-state analysis of an interleaved boost converter with coupled inductors," *IEEE Trans. Ind. Electron.*, vol. 47, no. 4, pp. 787–795, Aug. 2000.
 - [26] I. C. Trelea, "The particle swarm optimization algorithm: Convergence analysis and parameter selection," *Inf. Process. Lett.*, vol. 85, pp. 317–325, 2002.
- K. L. Lian** (M'07) received the B.A.Sc. (Hons.), M.A.Sc., and Ph.D. degrees in electrical engineering from the University of Toronto, Toronto, ON, Canada, in 2001, 2003, and 2007, respectively.
- He was a Visiting Research Scientist with the Central Research Institute of the Electric Power Industry in Japan from October 2007 to January 2009. He is currently an Assistant Professor with the National Taiwan University of Science and Technology, Taipei City, Taiwan.
- J. H. Jhang** received the B.S. degree from the National Taiwan University of Science and Technology, Taipei, Taiwan, in 2012, where he is currently working toward the M.S. degree.
- I. S. Tian** received the B.S. and M.S. degrees from the National Taipei University of Science and Technology, Taipei, Taiwan, in 2010 and 2012, respectively.
- He is currently with MiTAC International Corp., Taipei, Taiwan.